Assessment of NeQuick Ionospheric Model for Galileo single-frequency users

Antonio ANGRISANO, Salvatore GAGLIONE, Ciro GIOIA, Marco MASSARO, and Umberto ROBUSTELLI

Department of Applied Sciences – PArthenope Navigation Group (PANG)

"Parthenope" University of Naples, Italy

email: salvatore.gaglione@uniparthenope.it (corresponding author)

A b s t r a c t

The ionosphere is the main error source in GNSS measurements and in extreme cases can degrade significantly the positioning with errors exceeding 100 m; therefore modelling and predicting this type of error is crucial and critical. The ionospheric effect can be reduced using different techniques such as dual-frequency receiver or suitable augmentation system (DGPS, SBAS); the aforesaid approaches involve the use of expensive devices and/or complex architectures. Single frequency stand-alone receivers are the cheapest and most widespread GNSS device; they can estimate and partially correct the error due to the ionosphere, through adequate algorithms, which use parameters broadcasted by the navigation message. The aim of this paper is performances assessment of the ionospheric model NeQuick, adopted by the European GNSS Galileo for single frequency receivers. The analysis is performed in measurements domain and the data are collected in different geographical location and in various geomagnetic conditions.

Key words: GNSS, Galileo, Ionospheric Models, NeQuick, Klobuchar.

1. INTRODUCTION

GNSS (Global Navigation Satellite System) provide, with global coverage and in all weather conditions, three-dimensional position, velocity and time synchronization for users equipped with a receiver/processor (Hoffmann-Wellenhof et al. 1992, Kaplan and Hegarty 2006). The accuracy of GNSS depends on: observables accuracy, satellite geometry, number of tracked satellites and operational scenario.

To achieve a good positioning, raw pseudorange measurement must be corrected for the satellite clock error, relativistic effects, Sagnac effect and atmospheric delays, according to the following equation:

$$\rho_C = \rho + cdt_S + cdt_r + cdt_{Sag} - cdt_R - d_{Iono} - d_{Tropo} \quad (1)$$

where

ρ_C is the corrected pseudorange measurement,

ρ is the raw pseudorange measurement,

cdt_S is the satellite clock bias including TGD (Time Group Delay),

cdt_r is the relativistic effect correction term,

cdt_{Sag} is the delay due to the Sagnac Effect,

d_{Iono} is the ionospheric delay,

d_{Tropo} is the tropospheric delay and

c is the speed of light.

The table 1 (Parkinson 1996) quantifies the main error due to each above-mentioned sources.

Table 1. Statistical ranging error budget for GNSS single-frequency receiver.

Error Source	1σ error [m]
Ephemeris Data	2.1
Satellite Clock	2.1
Ionosphere	4.0
Troposphere	0.7
Multipath	1.4
Receiver measurement	0.5
User Equivalent Range Error	**5.3**

Ionosphere is the ionized region of the upper atmosphere which extends from about 80 km to more than 1000 km where the density of free electrons and ions influences the propagation of electromagnetic radio frequency waves (Hargreaves 1992). It is one of the higher source of ranging error for GNSS single frequency receivers, consequently reducing this type of error is fundamental. The structure and properties of the ionosphere depend essentially on: solar activity, variations of earth’s magnetic field (geomagnetic field effect), movements of neutral ‘‘wind’’ in the upper atmosphere due to earth’s rotation, the effects of electrical current and ambient electrical fields, the density and the content of the atmosphere at different altitudes and geographical latitudes, and so on (Blaunstein and Plohotniuc 2008).

Different methods can be adopted to minimize the ionospheric effect:

- use of dual-frequency technique,
- use of augmentation system,
- use of ionospheric model.

The dual-frequency technique corrects the measurements with an estimation of ionospheric delay obtained by a linear combination of dual frequency pseudorange measures (this technique is referred to as Iono-free). This method is the most effective but it cannot be used in a single frequency receiver.

Alternatively GNSS receivers can obtain the ionospheric correction through augmentation systems (such as Differential GPS - DGPS, or Satellite Based Augmentation System - SBAS), based on differential corrections, computed by a single station or by a network, and broadcasted to the receivers via terrestrial radio link or satellite.

While Augmentation systems involve the use of complex architectures, the use of broadcast ionospheric models is cheaper and easy to be implemented in commercial single frequency receiver.

2. IONOSPHERIC MODELS

The most efficient way to correct the ionospheric effects is to combine simultaneous measurements in k different frequencies, reducing the ionospheric effects up to order k-1 (Petit and Luzum 2010). A well-known example is provided by the so-called “ionospheric-free” technique, combining GNSS observables at the two frequencies, removing the first order ionospheric effect. The first order effect is biggest and its magnitude belongs to [0.1 , 100 m] interval, while the second and third order effects are estimated typically to be respectively ~0-2 cm and ~0-2 mm at zenith (Bassiri and Hajj 1992).

In the future, with Galileo and modernized GPS (Global Positioning System), the ionospheric correction can be extended to second order using signal at three different frequencies.

Single frequency users have to correct as much as possible the first order ionospheric term, which account for more than 99.9% of the total ionospheric delays (Petit and Luzum 2010). All the ICA (Ionospheric Correction Algorithms), providing ionospheric delay estimation, start from the evaluation of the electron concentration (N_e) relative to the path from satellite to user. The first order ionospheric delay is related to the signal frequency f and to the STEC (Slant Total Electron Content), defined as the electron concentration along the path between the receiver R and satellite S, whose equation is below:

$$STEC = \int_R^S N_e dl \tag{2}$$

STEC depends on many variables, including long and short term changes in solar ionizing flux, magnetic activity, season, time of day, user location and observation direction (Klobuchar 1987).

The dispersive effect of the ionosphere on GNSS observables causes a code delays and a phase advances obtained from the equations:

$$\delta_{\rho I}(phase) = -\frac{40.3 \cdot STEC}{f^2} \tag{3}$$

$$\delta_{\rho I}(code) = +\frac{40.3 \cdot STEC}{f^2} \tag{4}$$

Where $\delta_{\rho I}$ is expressed in meters, STEC in TECu (TEC units; 1 TECu = 10^{16} el/m^2) and f in MHz. The value of 1 TECu for the L1 frequency (1575.42 MHz) generates a delay of 0.16 m.

STEC can be computed using different techniques, which allow to correct directly the single frequency observables. Many of them start from the VTEC (Vertical Total Electron Content) available on global or regional scale (Liu et al. 2011); from the VTEC values corresponding to the observation time, the STEC can be estimated by using ionospheric mapping function F as shown in equation below:

$$STEC = F \cdot VTEC \tag{5}$$

Some common sources of electron content are (Petit and Luzum 2010):

- Global VTEC maps computed by the International GNSS Service (IGS) from a global network of dual-frequency receivers;
- Regional VTEC models, which provide better accuracy, by means of a better temporal and spatial resolution, thanks to the availability of a dense permanent receivers network (e.g. for Japan, Europe or USA);
- Predicted VTEC models used by GNSS (Klobuchar model for GPS or NeQuick for the future Galileo system);
- Empirical standard ionospheric models, which are based on all available data sources such as the International Reference Ionosphere – IRI (Bilitza and Reinisch 2007) or Parameterized Ionospheric Model – PIM (Daniell et al. 1995).

In the next sections are analyzed and compared the NeQuick model, adopted by the Galileo system, and Klobuchar one, used by the GPS single-frequency receivers.

2.1. NeQuick model

NeQuick is a semi-empirical model that describes spatial and temporal variations of the ionospheric electron density. It is based on the Di Giovanni-Radicella (DGR) ionospheric profiler (Di Giovanni and Radicella 1990) and provides both vertical or slant electron content for any specified path (Hochegger et al. 2000, Radicella and Leitinger 2001).

NeQuick model uses the peaks of the three main ionospheric regions (E, F1, and F2) as anchor points (Radicella and Leitinger 2001; Leitinger et al. 2005). The electron density at any location is computed starting from the characteristic parameters such as peak electron density and peak height; STEC is computed by integrating TEC along the signal path.

NeQuick model is at basis of the real-time ionospheric correction model algorithm used for Galileo single-frequency positioning (Radicella and Leitinger 2001, Schluter et al. 2004, Nava et al. 2005).

The standard NeQuick (Fortran 77) source code is available at: http://www.itu.int/oth/R0A04000018/en.

Taking advantage of the increasing amount of available data, the NeQuick has been continuously updated with changes involved the formulation of some specific parameters (Di Giovanni and Radicella 1990, Radicella and Zhang 1995, Leitinger et al. 2005, Coïsson et al. 2006) although conceptual structure of the model remained unaltered. In this revised model, the NeQuick electron density above 100 km and up to the F2-layer peak (the bottomside region) is calculated by a modified DGR profile formulation given by the sum of five semi-Epstein layers (Rawer 1982) with modeled thickness parameters (Radicella and Zhang 1995), whereas in the topside (the region of the ionosphere above the F2-layer peak) the electron density is described by an only semi-Epstein layer with a height dependent thickness parameter (Hochegger et al. 2000) empirically determined (Coïsson et al. 2006, Radicella 2009). The complete analytical formulation of the bottomside region is (Nava et al. 2008):

$$N_{bottomside}(h) = \sum_{i=E,F_1,F_2} N_i(h) = N_E(h) + N_{F_1}(h) + N_{F_2}(h) \qquad (6)$$

where:

$$N_E(h) = \frac{4N_{max}^E}{\left[1+\exp\left(\frac{h-h_{max}^E}{B^E}\xi(h)\right)\right]^2}\exp\left(\frac{h-h_{max}^E}{B^E}\xi(h)\right) \qquad (7)$$

$$N_{F_1}(h)=\frac{4N_{max}^{F_1}}{\left[1+\exp\left(\frac{h-h_{max}^{F_1}}{B^{F_1}}\xi(h)\right)\right]^2}\exp\left(\frac{h-h_{max}^{F_1}}{B^{F_1}}\xi(h)\right) \tag{8}$$

$$N_{F_2}(h)=\frac{4N_{max}^{F_2}}{\left[1+\exp\left(\frac{h-h_{max}^{F_2}}{B^{F_2}}\right)\right]^2}\exp\left(\frac{h-h_{max}^{F_2}}{B^{F_2}}\right) \tag{9}$$

with

$$N_{max}^{F_2}=N_{max}F_2 \tag{10}$$

$$N_{max}^{F_1}=N_{max}F_1-N_{F_2}\left(h_{max}^{F_1}\right) \tag{11}$$

$$N_{max}^{E}=N_{max}E-N_{F_1}\left(h_{max}^{E}\right)-N_{F_2}\left(h_{max}^{E}\right) \tag{12}$$

where

$$N_{max}E=0.124\left(f_0^E\right)^2,\quad N_{max}F_1=0.124\left(f_0^{F_1}\right)^2,\quad N_{max}F_2=0.124\left(f_0^{F_2}\right)^2$$

are the E, F1 and F2 layer peak electron densities (in 10^{11} m^{-3}), respectively,

$$h_{max}^{E},\ h_{max}^{F_1},\ h_{max}^{F_2}$$

the E, F1 and F2 layer peak heights (in km), respectively,

$$B^{E},\ B^{F_1},\ B^{F_2}$$

the E, F1 and F2 layer thickness parameters (in km), respectively, and

$$\xi(h)=\exp\left(\frac{10}{1+2\left|h-h_{max}^{F_2}\right|}\right) \tag{13}$$

is a function that ensures a “fading out” of the E and F1 layers in the vicinity of the F2 layer peak in order to avoid secondary maxima around $h_{max}^{F_2}$ (Nava et al. 2008).

The topside model formulation is:

$$N_{topside}(h)=\frac{4\,N_{max}^{F_2}}{\left[1+\exp(z)\right]^2}\exp(z) \tag{14}$$

where

$$z = \frac{h - h_{max}^{F_2}}{B_{topside}^{F_2}\left[1 + \frac{12.5\left(h - h_{max}^{F_2}\right)}{100\,B_{topside}^{F_2} + 0.125\left(h - h_{max}^{F_2}\right)}\right]} \tag{15}$$

and

$$B_{topside}^{F_2} = k\,B_{bottomside}^{F_2} \tag{16}$$

with parameter k given by (Coïsson et al. 2006):

$$k = 3.22 - 0.0538\, f_0F_2 - 0.00664\, h_{max}^{F_2} + 0.113\frac{h_{max}^{F_2}}{B_{bottomside}^{F_2}} + 0.00257 R_{12}$$

and $h_{max}^{F_2}$(km), f_0F_2 (MHz) are the F2 layer peak parameters, $B_{bottomside}^{F_2}$(km) the thickness of the F2 bottomside and R_{12} the smoothed sunspot number. As inferred from the experimental data analysis, the restriction $k \geq 1$ is applied in the model.

NeQuick algorithm was originally developed to be used with monthly averaged solar flux index F10.7 (solar radio flux per unit frequency at a wavelength of 10.7 cm); so to use model in real time application such as GNSS ionospheric correction model, the monthly averaged F10.7 index must be replaced by a daily input parameter in order to take in account both daily variation of the solar activity and the user's local geomagnetic condition. This daily input parameter is the so-called effective ionization level (Az) expressed in sfu (solar flux unit - 10^{-22}[W][m^{-2}][Hz^{-1}]) (Azpilicueta et al. 2003). Thus Az plays the role of the solar activity information provided to the model in order to fit a specific dataset. For Galileo single frequency operation, daily Az values will be computed from STEC measurements, obtained during the previous 24 hours, performed within the ground segment. From the calculated Az at different station of ground segment the worldwide behaviour of Az parameter is defined by a second order polynomial (Schluter et al. 2004) and is a function of receiver location as follows:

$$Az(\mu) = a_0 + a_1\,\mu + a_2\,\mu^2 \tag{17}$$

where μ is MOdified DIPolar latitude (MODIP) and a_0, a_1, a_2 are coefficients, created by optimizing the NeQuick model to a set of global network of permanent stations and broadcasted to the users within the Galileo navigation message (SIS-ICD 2006), updated least once a day allowing them to run the model (Radicella et al. 2003, Bidaine et al. 2012). MODIP is obtained as (Rawer 1963):

$$\mu = \operatorname{atan}\frac{I}{\sqrt{\cos\varphi}} \qquad (18)$$

where φ is the geodetic latitude and I magnetic field inclination (the angle that a magnetic needle makes with the horizontal plane at any specific location) at the receiver position.

In order to overcome limited access to Galileo navigation message, in this research the Az parameter for every location and day is estimated through the Brent method optimization (Brent 1973). Hence the ionization level adopted in NeQuick ICA, relative to a defined location and day, is the one that minimize the sequence:

$$Az = \arg\min \sum_{i=1}^{n} \left| VTEC_{Reference} - VTEC_{NeQuick}(Az) \right|_i^2 \qquad (19)$$

where

$VTEC_{Reference}$ is computed from the 1-day predicted GIMs (Global Ionospheric Maps) provided by CODE (Center for Orbit Determination in Europe – www.aiub.unibe.ch) in IONEX (IONosphere EXchange) format (Schaer and Gurtner 1998),

$VTEC_{NeQuick}(Az)$ is the VTEC of NeQuick model and

n is the number of considered polynomial nodes.

In the procedure adopted, to economize computation time, modeled VTEC ($VTEC_{NeQuick}$) is computed for Az belong to [0, 209 sfu] with a discretization interval of 16 sfu instead of interval [64, 193 sfu] used for F10.7 in standard NeQuick (Fortran 77) source code (Memarzadeh 2009).

2.2. Klobuchar model

Ionospheric Klobuchar model is an algorithm developed, around the mid-70s by J.A. Klobuchar, for single-frequency satellite receivers to correct approximately 50% of ionospheric delay (Klobuchar 1987) and was designed based on the Bent model (Bent and Llewllyn 1973). It is defined as a single layer ionospheric model (SLM - Single Layer Model), because the ionosphere (i.e. its TEC) is assumed as concentrated in an infinitesimal layer, placed at an average altitude of 350 km from the Earth's surface.

In a SLM the STEC is calculated in a geographic point (Ionospheric Point - IP) obtained by the intersection between the propagation direction (ray path, also called Line Of Sight - LOS) and the average height of the ionosphere. The projection on the surface of the ionospheric point is the SIP (Sub-Ionospheric Point) showed in figure 1.

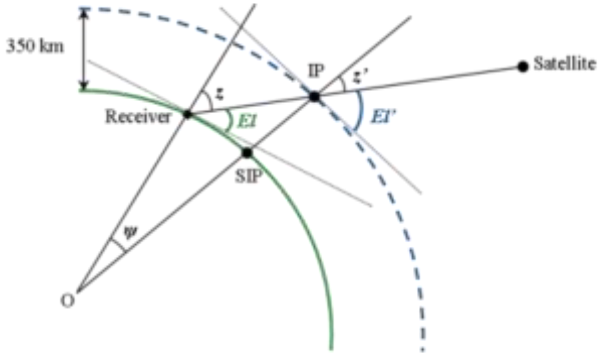

Figure 1. Klobuchar SLM.

Klobuchar model provides a different estimation for the daytime and nighttime ionospheric delay (in seconds) along the SIP vertical direction, starting from eight coefficients (transmitted in the navigation message) which describe the worldwide ionosphere behavior (Klobuchar 1987). Night time correction is assumed equal to a globally constant value (DC) of 5 ns (~ 1.5 m) for L1 carrier, while the diurnal vertical delay is modeled as cosine featured by: amplitude A, period P and phase Φ depending from the geo-magnetic latitude of SIP, according to:

$$T_{iono}^{V} = DC + A\cos\left[\frac{2\pi\left(t-\Phi\right)}{P}\right] \tag{20}$$

where T_{iono}^{V} is the vertical Ionospheric delay.

In order to compute A and P in any Earth position, eight coefficients (four α for A and four β for P) of two third-degree polynomials, are broad-casted daily in the GPS satellites navigation message. The GPS Ground Con-trol Segment updates these coefficients according to season and solar activity level. The phase Φ of the cosine function is constant and equal to 14 hours. When cosine argument [2π(t – Φ)/P], is greater than π/2 [rad] cosine function starts to be negative and T_{iono}^{V} is represented only by the DC term.

According to equation (5) the delay along LOS (T_{iono}) is computed by:

$$T_{iono} = F \cdot T_{iono}^{V} \tag{21}$$

where

$$F = 1 + 16 \cdot \left(0.53 - El\right)^{3} \tag{22}$$

Starting from a Taylor series approximation of the equation (20) the Klobuchar model general expression, for L1 carrier delay, is:

$$T_{iono} = \begin{cases} F \cdot \left[5 \cdot 10^{-9} + A \left(1 - \frac{x^2}{2} + \frac{x^4}{24} \right) \right] & \text{if } |x| \le 1.57 \\ F \cdot \left(5 \cdot 10^{-9} \right) & \text{if } |x| > 1.57 \end{cases} \quad (23)$$

3. TEST AND RESULTS

In order to verify the NeQuick model efficiency, its performances are compared with Klobuchar ones in measurement domain evaluating relative ionospheric delay error. Comparison algorithm process used is shown in figure 2. The main inputs are the GNSS (GPS) ephemerides, propagated to the transmission epoch by an orbital propagator (IS-GPS-200 2004), the coordinates of the considered stations and the predicted GIM (used for Az computation). The "Iono Delay Estimation" structure estimates the ionospheric delay using different models such as NeQuick and Klobuchar; the reference is computed using Final GIM produced by IGS. Finally, the estimated delays are compared with the reference and the model performances are analyzed in terms of error bias, STD (STandard Deviation), RMS (Root Mean Square) and relative error (defined as the ratio between bias and IGS GIM iono delay).

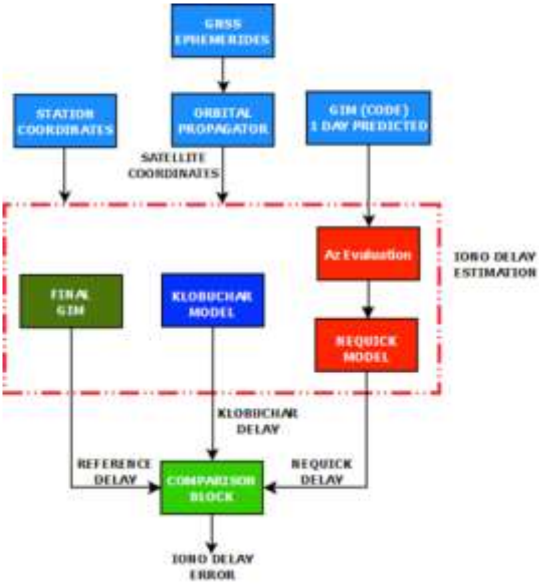

Figure 2. Comparison Algorithm.

All the software belong to a Toolbox developed by PANG (PArthenope Navigation Group – http://pang.uniparthenope.it) except for NeQuick model that is open and downloadable on ITU (International Telecommunication Union) web site.

In order to investigate spatial correlation of the models, ephemerides data in RINEX format, stored in stations placed at different latitudes and Earth hemisphere are processed.

Station coordinates are shown in next table and their global positions are shown in figure 3.

Table 2. Station details.

ID	City	Location	Latitude (deg)	Longitude (deg)	Height (m)
HOLM	Holman	Canada	N 70.7364	242.2391	39.5000
AREQ	Arequipa	Peru	S 16.4655	288.5072	2488.9226
PANG	Naples	Italy	N 40.8234	14.2161	122.6590
MCM4	Ross Island	Antarctica	S 77.8383	166.6693	98.0222
CEDU	Ceduna	Australia	S 31.8667	133.8098	144.8155

Figure 3. Station location.

For time correlation investigation, results are shown for several days in the years 2008-2010 featured by different geomagnetic activity that, as known, affects ionospheric activity.

In figure 4 the Ap (Average planetary) index - a daily Planetary-scale measure of magnetic activity (Menvielle and Berthelier 1991) - is plotted for the examination period. Circle tags indicate maximum Ap index relating to high geomagnetic activity.

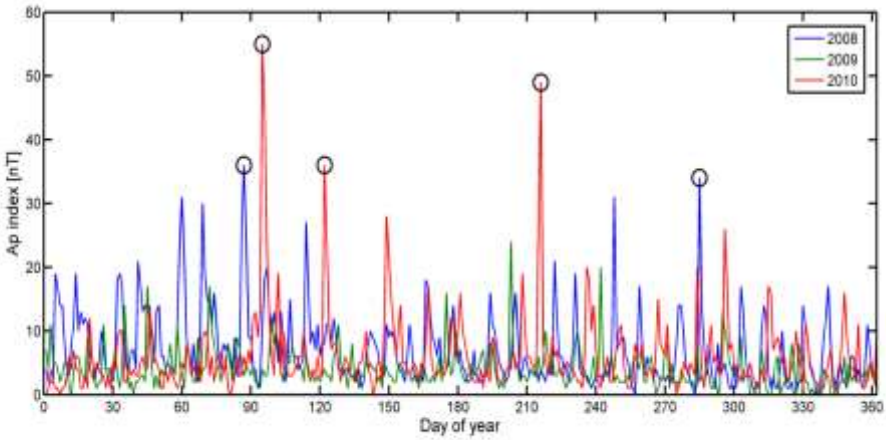

Figure 4. Ap index in the years 2008, 2009, 2010.

In table 3 the analyzed DOY (Day Of Year) are classified for relative Ap value, related to geomagnetic activity.

Table 3. Summary of Ap index in DOY under test.

Geomagnetic Activity	Ap index	DOY/YEAR
Light	0	257/2008
	0	316/2009
	1	016/2010
	1	344/2010
Medium	18	032/2008
	16	194/2008
	16	175/2009
	26	296/2010
High	36	087/2008
	34	285/2008
	55	095/2010
	36	122/2010
	49	216/2010

3.1. Measurement Domain Analysis

To make an assessment between the aforesaid models, it is necessary to identify a reference for error analysis; in measurement domain it is provided by IGS final GIM, evaluated from iono-free solution of post processing data stored in IGS stations.

Figure 5 and figure 6 are related to the PANG data processing for 16/2010 day. The iono delay for two GPS satellites (SAT2 and SAT11) are plotted versus satellite elevation (left diagram of figures 5 and 6) and versus UTC (Coordinated Universal Time) (right diagram of figures 5 and 6). For satellite 2, as expected, Klobuchar model provides same correction for different tracking (one had in the morning and one in the afternoon) while NeQuick and GIM have two different trends. For satellite 11 occurred only one daily track; in both cases Klobuchar delay is bigger.

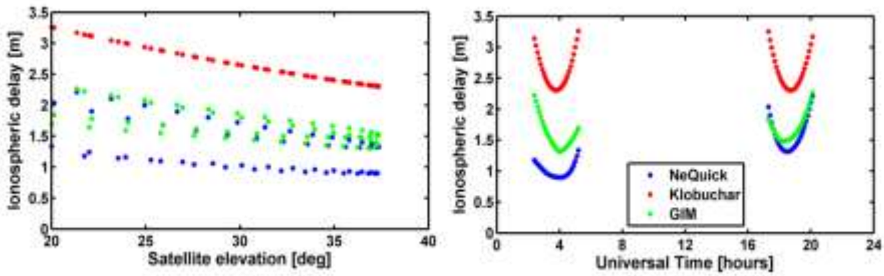

Figure 5. Ionospheric delay vs elevation and UT for SAT2 at PANG on 16/2010.

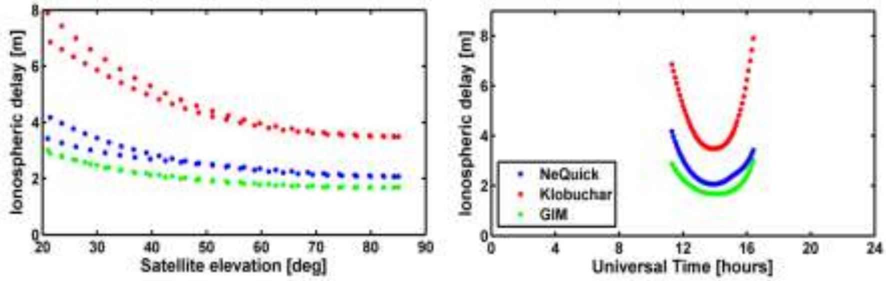

Figure 6. Ionospheric delay vs elevation and UT for SAT11at PANG on16/2010.

Figure 7 and figure 8 show results relative to two different stations (HOLM and AREQ) for all tested days. In figure 7 the relative delays for the two models and the reference are plotted versus satellite elevation .It can be noted that ionospheric delays computed are bigger for the equatorial station AREQ, according to theory.

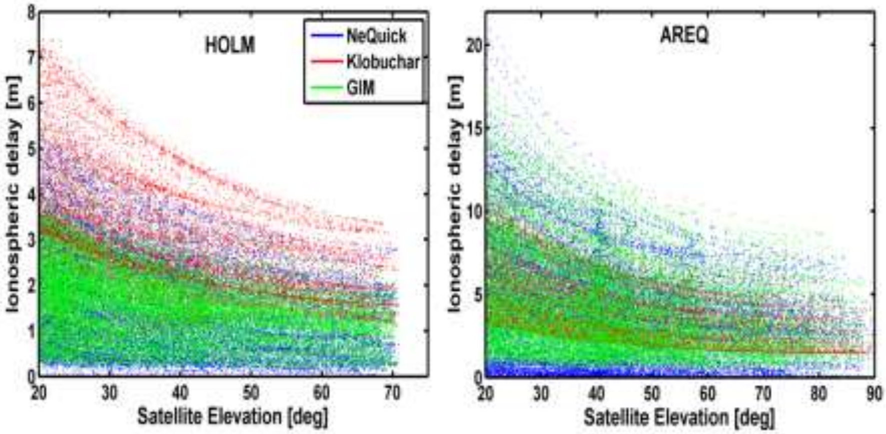

Figure 7. Ionospheric delay vs satellite elevation for HOLM and AREQ in all days tested.

From the figure above it can be seen how change the ionospheric delay respect satellite elevation. It can be noted clearly how as it increases with the reduce of elevation.

In figure 8 delays for two models and reference are plotted versus UTC with same three color lines meaning. It can be noted that ionospheric delay has two different maximum, higher for the equatorial station AREQ, at middle of day in local times (12:00 – 16:00 local times, 17:00 – 21:00 UTC) when maximum ionospheric activity is expected.

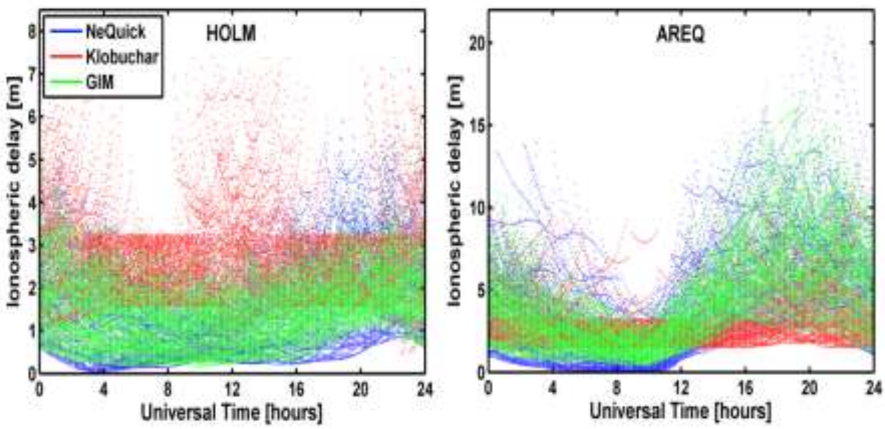

Figure 8. Ionospheric delay vs UT for HOLM and AREQ in all days tested.

In Figure 9 and 10 two models are compared with respect to the reference. NeQuick iono delay estimation is characterized by an absolute error distribution more close to zero mean testifying its efficiency. From figure 9, representing the errors with respect to the satellite elevation, it can be noticed that higher model errors are relative to low satellite elevation.

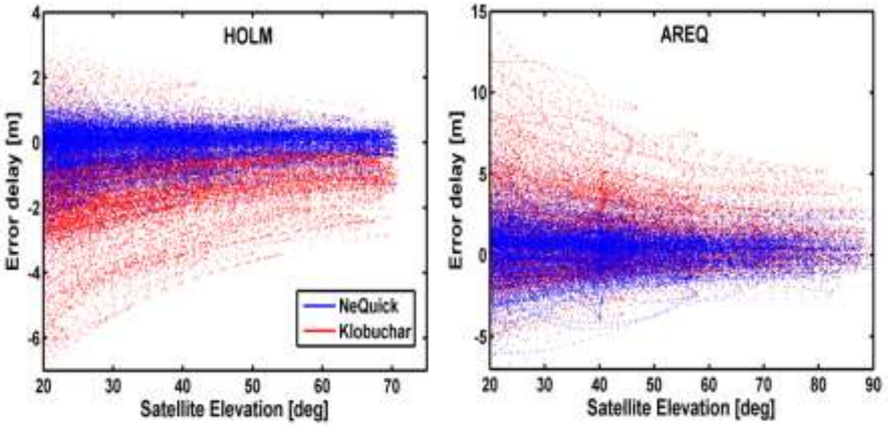

Figure 9. Differences between GIM and Models vs satellite elevation for HOLM and AREQ for all days tested.

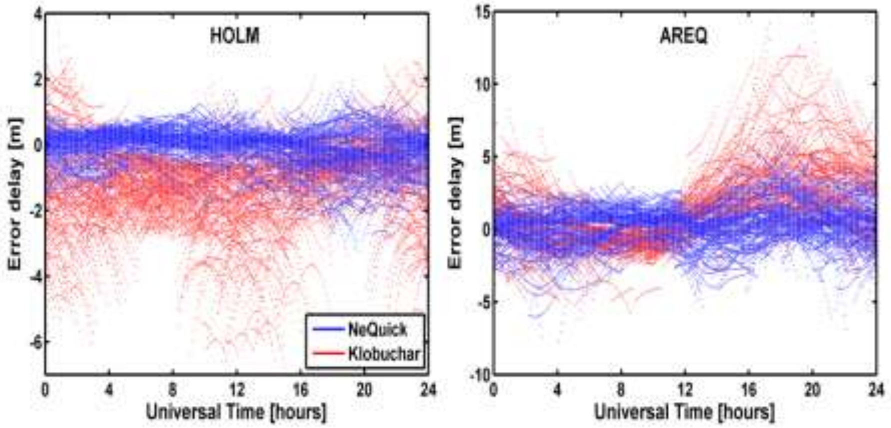

Figure 10. Differences between GIM and Models vs UT for HOLM and AREQ for all days tested.

The figures 9 and 10 are the most significant. They show difference between ionospheric estimation achieved by models and GIMs for all day tested, as a function of the satellite elevation (figure 9) and the Universal Time (figure 10). They show a greater overestimation of Klobuchar ionospheric delay for Holman polar station (red point in left subfigure) and an underestimation for equatorial station Arequipa (right subfigure). Moreover equatorial station shows a greater error delay: in fact, while in Holman station Klobuchar higher error in absolute value is equal to 6.5 meters, in Arequipa error reaches a maximum value of 15 meters. NeQuick model delay estimation has, instead, a more regular trend with a daily variation around the zero.

In figure 11 a statistical analysis summary for HOLM data processed is shown considering days characterized by different geomagnetic activity (see table 3). The results are compared in terms of: error bias, standard deviation, RMS and relative error (defined as the ratio between bias and IGS GIM iono delay, it is dimensionless).

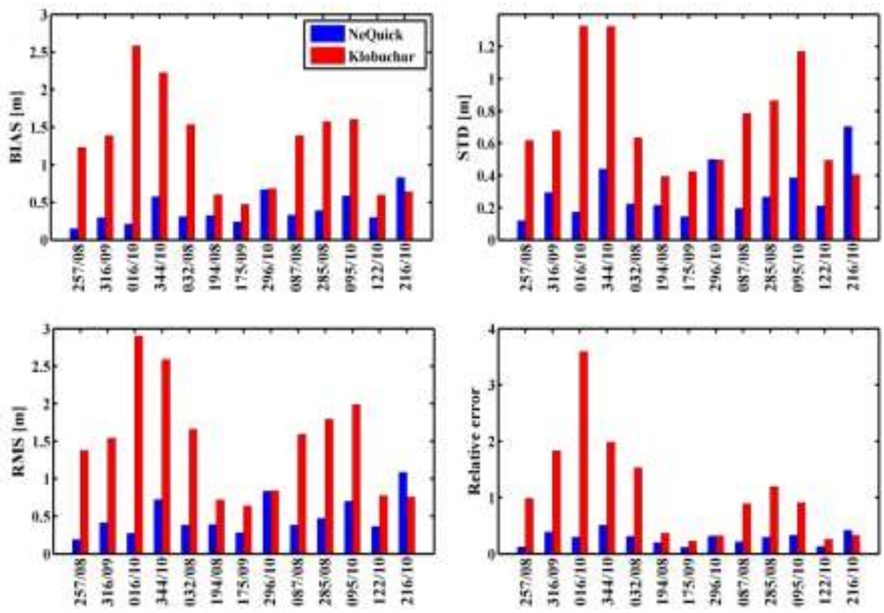

Figure 11. HOLM Statistical Results.

Unexpected results occurred in 2 days: one of medium activity (296/10) and one of heavy condition (216/10). Two models gave same results on 296/10 or a better solution for Klobuchar occurred on 216/10.

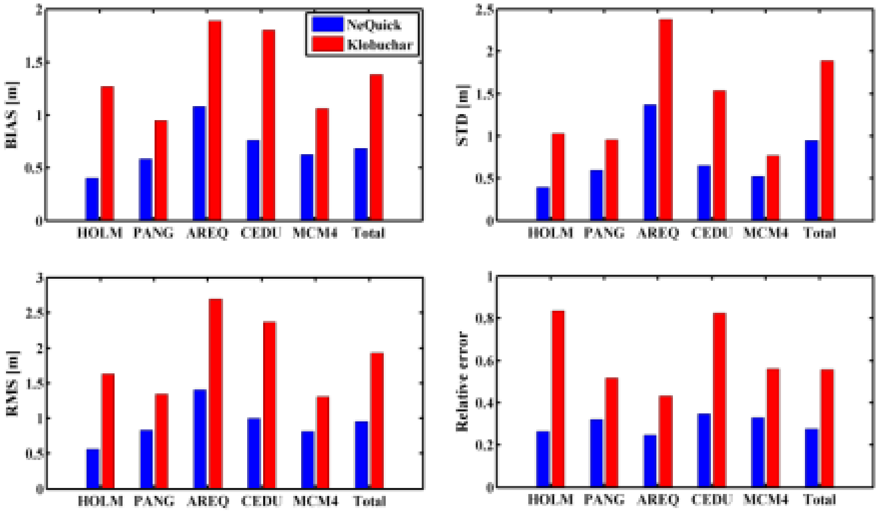

Figure 12. Global Results: Statistical comparisons.

For a qualitative analysis, all statistical parameters are plotted in Figure 12 over all the studied days (thirteen) and for all stations and the results are summarized in table 4.

Table 4. Summary results.

STATION	BIAS NeQuick [m]	BIAS Klobuchar [m]	STD NeQuick [m]	STD Klobuchar [m]	RMS NeQuick [m]	RMS Klobuchar [m]
HOLM	0.3995	1.2685	0.3895	1.0265	0.5579	1.6318
PANG	0.5816	0.9445	0.5927	0.9541	0.8304	1.3425
AREQ	1.0783	1.8881	1.3710	2.3758	1.4056	2.6905
CEDU	0.7576	1.7988	0.6473	1.5352	0.9965	2.3648
MCM4	0.6215	1.0595	0.5211	0.7658	0.8111	1.3073

The results summarized in figure 12 and in table above, show the behaviour of the considered models; NeQuick guarantees more accurate estimation of the ionospheric delay with respect to Klobuchar. The performances are improved in terms of bias, STD, RMS and relative error for all analyzed stations. Best statistical index are related to the Canadian station HOLM while for equatorial region AREQ iono delay evaluation is less accurate.

4. CONCLUSIONS

Based on the research results presented in this paper, NeQuick ionospheric delays in zenithal direction for the L1 frequency belong to the interval [1-4.5 m] with a maximum value of about 8 meters in equatorial region;

while for the low elevation angle ~20° the maximum value is 20 meters for an equatorial station and the average delay belongs to the interval [2-9 m]. The maximum NeQuick ionospheric delay error vary from 2 (for polar stations) to 4 meters (for equatorial stations) in zenith direction and from 3 to 7 meters for low elevation satellites, while the Klobuchar achieves a worse performance with maximum errors between 4 (for polar stations) and 5 meters (for equatorial stations) in the zenith direction and from 7 to 15 meters for low elevation satellites. In accordance with theory, test results in time domain have highlighted that the NeQuick ionosphere delays variation have a daily maximum close to the 14:00 local time while the spatial analysis have showed that its behavior increases at lower latitudes. According to the analysis results of different geomagnetic activity, it is noted that the Klobuchar relative error is maximum for the period of low geomagnetic activity. Instead the NeQuick one is much lower and constant around the value of 27% (26.61% for light, 28.68% for medium and 27.24% for high geomagnetic activity). In fact the NeQuick average relative error for all day tested and all stations is 27.47% while for Klobuchar model the mean relative error is 55.71% and therefore the NeQuick model halves the relative error of the Klobuchar one.

Finally two models comparison has shown how NeQuick model has better performances than Klobuchar one. In 98% of tests, Galileo model has provided a better ionospheric delay estimation.

5. FUTURE WORK

The authors studies will be focused on the Use of Ionization Level Az as provided from Galileo Navigational Message and on further investigation in position domain.

ACKNOWLEDGMENTS

The authors wish to acknowledge Sandro M. Radicella Head Aeronomy and Radiopropagation ICTP Laboratory (Trieste, Italy) who gave a useful guide.

References

Angrisano, A., S. Gaglione, C. Gioia, U. Robustelli, and M. Vultaggio (2012), GIOVE Satellites Pseudorange Error Assessment, Journal of Navigation 65, 29-40, DOI: 10.1017/S0373463311000270.

Aragón-Ángel, A., R. Orús, M. Hernández-Pajares, J. M. Juan, and J. Sanz (2006), Preliminary NeQuick Assessment for future single frequency users of Galileo. In: Proc. Of the 6th Geomatic week, Barcelona, Spain.

Arbesser-Rastburg, B. (2006), The Galileo Single Frequency Ionospheric Correction Algorithm, 3rd European Space Weather Week, Brussels, Belgium, 16/11/2006.

Azpilicueta, F., P. Coïsson, B. Nava, C. Brunini, and S. M. Radicella (2003), Optimized NeQuick ionospheric model for point positioning. In: Proc. of Inter. Symposium on GPS/GNSS, 15-18 Nov. 2003, Tokyo, Japan.

Bassiri, S. and G.A. Hajj (1992), Modeling the GPS Signal Propagation Through the Ionosphere, TDA Progress Report 42-110, August 1992.

Bent, R. B. and S. K. Llewllyn (1973), Documentation and Description of the Bent Ionospheric Model, SAMSO Technical Report, 73-252.

Bidaine, B., M. Lonchay and R. Warnant (2012), Galileo Single Frequency Ionospheric Correction: Performances in Terms of Position, GPS Solutions April 2012, DOI: 10.1007/s10291-012-0261-0.Bilitza, D. and B. Reinisch (2007), International Reference Ionosphere 2007: Improvements and new parameters, J. Adv. Space Res., 42(4), 599-609, DOI: 10.1016/j.asr.2007.07.048.

Blaunstein, N. and E. Plohotniuc (2008), Ionosphere and Applied Aspects of Radio Communication and Radar, CRC Press, Taylor & Francis Group.

Brent, R. P. (1973). Algorithms for Minimization without Derivatives, Prentice-Hall, Englewood Cliffs, New Jersey.

Coïsson, P., S.M. Radicella, R. Leitinger, B. Nava (2006), Topside electron density in IRI and NeQuick: features and limitations. In: Advances in Space Research (37), 937-942.

Daniell, R. E., L. D. Brown, D. N. Anderson, M. W. Fox, P. H. Doherty, D. T. Decker, J.J. Sojka, and R.W. Schunk (1995), Parameterized Ionospheric Model: A global ionospheric parameterization based on first principles models. In: Radio Sci., 30(5), 1499-1510, DOI: 10.1029/95RS01826.

Di Giovanni, G. and S. M. Radicella (1990), An analytical model of the electron density profile in the ionosphere, Advances in Space Research, Volume 10, no. 11, 27-30, DOI: 10.1016/0273-1177(90)90301-F.

Hargreaves, J.K. (1992), The solar-terrestrial environment. In: Cambridge Atmospheric and Space Science Series, Cambridge University Press.

Hochegger, G., B. Nava, S. M. Radicella, and R. Leitinger (2000), A family of ionospheric models for different uses, Physics And Chemistry Of The Earth, Volume 25, N. 4, 307-310, DOI: 10.1016/S1464-1917(00)00022-2.

Hoffmann-Wellenhof, B., H. Lichtenegger, and J. Collins (1992), Global Positioning System: Theory and Practice, Springer, Inc.

IS-GPS-200 (2004), Navstar GPS Space Segment/Navigation User Interfaces, Revision D, ARINC Research Corporation, El Segundo, CA.

Kaplan, E. D., and C. J Hegarty (2006), Fundamentals of Satellite Navigation. Understanding GPS: Principles and Applications. In: E. D. Kaplan, and C. J Hegarty (eds.), 2nd ed. Artech House, Inc., Norwood, MA, 21-65.

Klobuchar, J. A. (1987), Ionospheric time-delay algorithm for single-frequency GPS users, IEEE Transactions on aerospace and electronic systems, Volume AES- 23, N. 3, 325-331.

Leitinger, R., Zhang, M. L. and Radicella, S. M. (2005), An improved bottomside for the ionospheric electron density model NeQuick, Annals of Geophysics, Volume 48, N. 3, 525-534, DOI: 10.4401/ag-3217.

Liu, J., Chen, R., Wang, Z. and Zhang H. (2011), Spherical cap harmonic model for mapping and predicting regional TEC, GPS Solutions, 15(2), 109-119.

Massaro, M. (2011), Confronto tra modelli ionosferici nel posizionamento GNSS in singola frequenza, Master Degree thesis, "Parthenope" University of Naples.

Memarzadeh, Y. (2009), Ionospheric modeling for precise GNSS applications, PhD thesis, Delft University of Technology.

Menvielle, M., and A. Berthelier (1991), The K-derived planetary indices - description and availability, Reviews of Geophysics, 29, 415–432, DOI: 10.1029/91RG00994.

Nava, B., P. Coïsson, G. M. Amarante, F. Azpilicueta, and S. M. Radicella (2005), A model assisted ionospheric electron density reconstruction method based on vertical TEC data ingestion, Annals of Geophysics, Vol. 48, N. 2, DOI: 10.4401/ag-3203.

Nava, B., P. Coïsson and S.M. Radicella (2008), A new version of the NeQuick Ionosphere electron density model. In: Journal of Atmospheric and Solar Terrestrial Physics 70(2008), 1856-1862.

Parkinson, B. W. (1996), GPS Error Analysis. In: B. W. Parkinson, and J. J. Spilker, Global Positioning System: Theory and Applications, American institute of Aeronautics and Astronautics, Inc., Washington, DC, 469-483.

Petit, G. and B. Luzum (2010), IERS Conventions (2010). In: G. Petit, and B. Luzum (eds.), IERS Technical Note No. 36, Verlag des Bundesamts für Kartographie und Geodäsie, Frankfurt, Germany, 137-150.

Radicella, S. M. (2009), The NeQuick model genesis, uses and evolution, Annals of Geophysics, Vol. 52, N. 3/4, June/August 2009, 417-422.

Radicella, S. M. and R. Leitinger (2001), The evolution of the DGR approach to model electron density profiles, Advances in Space Research, Volume 27, 35–40, DOI: 10.1016/S0273-1177(00)00138-1.

Radicella, S.M., B. Nava, P. Coïsson and R. Leitinger (2003), A Flexible 3D Ionospheric Model for Satellite Navigation Applications. In: International Symposium on GPS/GNSS, Japan 2003, pp. 305 - 310.

Radicella, S.M. and M.L. Zhang (1995), The improved DGR analytical model of electron density height profile and total electron content in the ionosphere. In: Annali di Geofisica XXXVIII (1), 35–41.

Rawer, K. (1963), Meteorological and Astronomical Influences on radio Wave Propagation, Pergamon Press, Inc.

Rawer, K. (1982), Replacement of the present sub-peak plasma density profile by a unique expression. In: Advances in Space Research 2(10), 183-190.

SIS-ICD (2006), Galileo Open Service, Signal In Space Interface Control Document, SISICD-2006. European Space Agency.

Schaer, S and W. Gurtner (1998), IONEX: The IONosphere Map Exchange, Format Version 1. In: Proc. of the IGS AC Workshop, Darmstadt, Germany, February 9-11, 1998.

Schluter, S., Y. Beniquel, C. Bourga, B. Arbesser-Rastburg, N. Jakowski, F. Amarillo, D. Klahn, and T. Noack, (2004), Ionosphere related contribution of the atmospheric processing and assessment facility to gstb-v1. In: Proc. of The European Navigation Conference 2004, 16-19 May, Rotterdam, The Netherlands.